Structural manipulation of the photocatalytic activity of TiO$_2$ nanotube arrays

Chan Lin, Lixin Cao and Shaowei Chen

Published by:

$\circledS$SAGE

http://www.sagepublications.com

On behalf of:

Institution of MECHANICAL ENGINEERS

Institution of Mechanical Engineers

>> Version of Record - Nov 13, 2014

OnlineFirst Version of Record - Nov 8, 2013

What is This?

Original Article

Structural manipulation of the photocatalytic activity of TiO$_2$ nanotube arrays

Chan Lin[1,2], Lixin Cao[3] and Shaowei Chen[2]

Abstract

Highly ordered TiO$_2$ nanotube arrays on Ti substrates were prepared by an electrochemical anodization process in a mixture of glycerol and water containing 0.5 wt% NH$_4$F and then thermally annealed from 400 °C to 600 °C. The sample structures were characterized by scanning electron microscopy and X-ray diffraction measurements, where the nanotube pore diameter and length were found to increase with increasing anodization voltage and reaction time. Thermal annealing at 450 °C was found to lead to the generation of the largest anatase crystalline domains, and at higher annealing temperature, the anatase components started to convert into the rutile ones. The corresponding photocatalytic activity was then evaluated by the photodegradation of Alizarin Red S under ultraviolet light irradiation. The results showed that the nanotubes prepared by anodization at 25 V for 10 h and subsequently annealed at 450 °C exhibited the optimal photocatalytic activity with a rate constant of $2.70 \times 10^{-3} \, min^{-1}$ and 39.2% of Alizarin Red S degraded after 180 min of photoirradiation. These results indicated that the photocatalytic activity was primarily determined by the crystalline properties of the TiO$_2$ nanotubes, and additional improvement might be achieved by a deliberate manipulation of the nanotube dimensions as a combined contribution of light penetration and mass transport within the nanotube arrays.

Introduction

With the development of the textile industries, large amounts of wastewater containing organic pollutants are being discharged into the environment. Thus, a number of procedures have been developed in recent years in order to mitigate the detrimental impacts of these pollutants on the environment. Among these, photocatalysis represents an effective method.[1–4] Of the photocatalysts used, TiO$_2$ has drawn considerable attention primarily because of its low cost, nontoxicity, and apparent photocatalytic efficiency. In practice, to maximize surface accessibility, the catalysts are prepared in the form of nanostructures. In fact, a variety of procedures have been developed for the fabrication of these functional nanostructures. For instance, one-dimensional TiO$_2$ nanotubes have been synthesized by the template method,[5] hydrothermal route,[6] electrochemical anodization,[7] and microwave irradiation.[8] Among these, highly oriented TiO$_2$ nanotube arrays prepared by electrochemical anodization have shown excellent catalytic activity for the degradation of organic pollutants due to its high surface-to-volume ratios, dispersibility, and fast charge transfer properties.[7]

Yet, most anodically prepared TiO$_2$ nanotube arrays are amorphous with poor conductivity and mechanical strength.[9] For photocatalytic applications, the crystallinity of the TiO$_2$ nanotube arrays must be improved, where thermal annealing has been recognized as a feasible and effective route.[10] In addition, the nanotube length and pore size may also influence the photocatalytic activity as

[1]College of Chemistry and Chemical Engineering, Ocean University of China, Shandong, People's Republic of China
[2]Department of Chemistry and Biochemistry, University of California, Santa Cruz, CA, USA
[3]Institute of Materials Science and Engineering, Ocean University of China, Shandong, People's Republic of China

Corresponding author:
Shaowei Chen, Department of Chemistry and Biochemistry, University of California, 1156 High Street, Santa Cruz, CA 95064, USA.
Email: shaowei@ucsc.edu

a result of effective surface area and diffusion of reactants and reaction products. For instance, Kang and Chen[11] thermally annealed TiO$_2$ nanotube arrays from 400 °C to 600 °C and found that the nanotubes prepared at 500 °C exhibited the maximal photocatalytic activity in the degradation of methylene blue because of the formation of a binary mixture of anatase and brookite crystalline phases that facilitated charge separation upon photoirradiation. In another study, Yu and Wang[12] studied the influence of annealing temperature on the TiO$_2$ structures and found that the photocatalytic activity in the degradation of methyl orange increased with increasing temperature, and at 600 °C, the annealed sample displayed the highest photocatalytic activity due to its anatase and rutile biphasic composition, good crystallization, and remaining tubular structures. In a further study, Lai et al. examined the effects of TiO$_2$ nanotube length and annealing temperature on the efficiency of photodegradation of methyl orange. It was found that when calcined at 450 °C, the nanotubes of 2.5 μm in length showed the best photocatalytic activity.[13] All these studies highlight the significance of the TiO$_2$ crystalline composition in the manipulation of the photocatalytic activity. Yet the discrepancy among these studies also suggests that other structural parameters might impact the nanotube photocatalytic activity, such as surface morphologies, tubular length, pore diameter, and so on. This is the primary motivation of the present study.

In this article, highly ordered TiO$_2$ nanotube arrays were fabricated by the anodic oxidation of a titanium metal sheet. The photocatalytic activity of the TiO$_2$ nanotube arrays was examined within the context of various structural parameters that included pore size, tube length, and crystallographic composition. As a representative highly toxic anthraquinone compound dye with a high chemical oxygen demand value (Figure 1), Alizarin Red S (ARS) was used as a model pollutant to evaluate and compare the photocatalytic activity of these TiO$_2$ nanotube arrays under ultraviolet (UV) illumination, from which the optimal experimental conditions were identified for the preparation and engineering of the TiO$_2$ nanotubes.

Experimental section

Preparation of TiO$_2$ nanotube arrays

Titanium (Ti) foils (250 μm in thickness, 99.5% purity) were purchased from Alfa-Aesar, USA. Prior to anodization, a large piece of a Ti foil was cut into small rectangular pieces of 15 mm × 10 mm. These Ti pieces were then ultrasonically cleaned in acetone and anhydrous ethanol for 20 and 10 min, respectively, then rinsed several times with deionized water, and dried in a nitrogen stream. TiO$_2$ nanotube arrays were fabricated by the electrochemical anodization method, which was conducted in a conventional two-electrode configuration under magnetic agitation.[11] A titanium foil and a graphite sheet served as the anode and cathode,
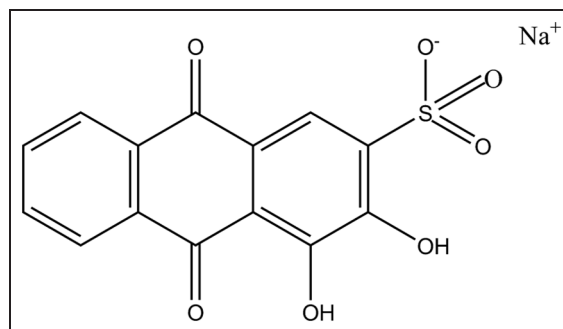

Figure 1. Molecular structure of Alizarin Red S (ARS).

respectively. These electrodes were separated with a distance of 4 cm and submerged into an electrolyte solution of glycerol and water (at a glycerol/water volume ratio of 4:1) containing 0.5 wt% NH$_4$F. The applied voltage was controlled by using a direct current (DC) power supply (Full Electric Co. Ltd., China). The electrochemical treatment started with a potential ramp from the open-circuit potential to a designated voltage at a scan rate of 0.1 V/s, followed by holding the applied potential for various periods of time. After anodization, the samples were rinsed with deionized water and dried in a nitrogen stream. All experiments were carried out at room temperature.

Characterization

The morphology of the TiO$_2$ nanotube arrays was characterized by using a Hitachi S-4800 field emission scanning electron microscope (FESEM). The cross-sectional images were taken from cracked layers after mechanical bending of the samples. The crystalline phases were determined by X-ray diffraction (XRD) studies using a Bruker D8 Advance X-ray diffractometer fitted with Cu K$_\alpha$ radiation over the 2θ range of 20° to 70° at a scanning speed of 5°/min.

Photocatalysis

The photocatalytic activity of TiO$_2$ nanotube arrays was examined by the degradation of ARS in aqueous solutions at ambient temperature with an OCRS-I photochemical reactor (Kaifeng Hongxing Machinery and Electronics Co., Henan, China). The experimental setup is shown in Figure 2. A 300-W high-pressure mercury lamp was used as the light source, which was put in a cylindrical quartz cooling pit with circulating water. The initial concentration of the ARS solution was 40 mg/L, and the solution pH was adjusted by NaOH solution to 9. At the beginning of the reaction, 10 mL of an ARS solution was added into a 25-mL quartz beaker. A calculated amount of photocatalysts was loaded into the solution with the TiO$_2$ nanotube arrays facing the lamp. The distance between the quartz beaker and the lamp was 10 cm. Prior to photoirradiation, the photocatalysts were soaked in the ARS solution for 30 min in the dark to establish an adsorption–desorption equilibrium. A magnetic stirrer
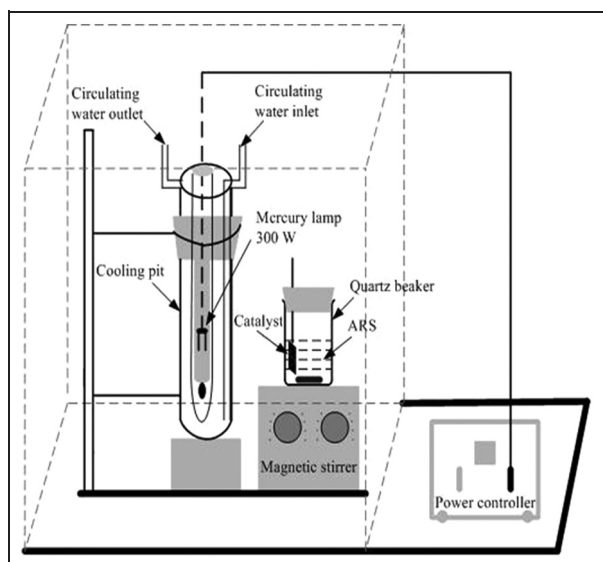
Figure 2. Experimental setup for photocatalytic reactions.

was used to ensure a good mixing during the entire process. After different reaction intervals, an aliquot of the ARS solution was taken out from the beaker for UV-vis absorption measurements (Shimadzu UV-2550, Japan). The photodegradation activity was measured by the change of the peak absorbance at about 520 nm with respect to that prior to light exposure. Control experiments were also carried out by irradiating the ARS solution without TiO_2 photocatalysts under the otherwise identical conditions.

Results and discussion

Figure 3 shows the top and cross-sectional views of TiO_2 nanotube arrays prepared at different anodization voltages and times. It can be seen that the TiO_2 nanotube arrays are all rather uniform in size in each sample and tightly packed on the Ti foil surface. Yet a closer analysis shows that the detailed structures of the nanotube arrays vary with the experimental conditions. For instance, for a reaction time of 2 h, with the increase of the anodization voltage, the outer diameter of the TiO_2 nanotubes exhibited an apparent increase, from approximately 120 nm at 25 V (panel a) to 150 nm at 35 V (panel b) and finally 185 nm at 45 V (panel c), whereas the tube number density decreased from about 58 to 31, and to 19 per μm^2, respectively. Nonetheless, the tube thickness remained rather consistent at about 10 nm. In addition, the length of the TiO_2 nanotube arrays might be varied by the reaction time, as manifested in the cross-sectional views of the nanotube arrays. For instance, at the same anodization voltage of 25 V, the length of the TiO_2 nanotube arrays was found to increase almost linearly with increasing reaction time, from about 0.90 μm for 2 h (panel d) to 2.75 μm for 10 h (panel e) and 3.76 μm for 12 h (panel f). At a higher anodization voltage of 35 V, the average length was even longer, and also increased linearly with reaction

time, from 1.19 μm for 2 h (panel g) to 3.40 μm for 8 h (panel h) and 4.34 μm for 12 h (panel i). Interestingly, a further increase of the anodization voltage did not appear to lead to a significant change of nanotube length. For instance, at 45 V, the average TiO_2 nanotube length was about 1.50 μm for 2 h (panel j), 3.07 μm for 6 h (panel k), and 3.96 μm for 12 h (panel l).

The resulting nanotube arrays were then subject to thermal annealing between 400 °C and 600 °C to manipulate the crystalline structures, as revealed by XRD measurements.[11,12,14] Figure 4 depicts the representative XRD patterns of TiO_2 nanotube arrays prepared at 25 V with the anodization time of 10 h (a) before and after thermal annealing at (b) 400 °C, (c) 450 °C, (d) 500 °C, (e) 550 °C, and (f) 600 °C. It can be seen that the as-prepared TiO_2 nanotube arrays (curve a) exhibited a largely featureless profile (the sharp diffraction features at 35.09°, 38.39°, 40.16°, 52.98°, and 62.94° were due to the Ti metal substrate), implying an amorphous structure. After annealing at 400 °C in air for 3 h (curve b), several diffraction peaks appeared at 25.28°, 48.05°, and 55.06°, which were consistent with the (101), (200), and (211) crystalline planes of anatase TiO_2, respectively. When the annealing temperature was increased up to 550 °C (curves c to e), these diffraction peaks became increasingly sharpened, suggesting an increase of the TiO_2 crystallinity. Interestingly, at the annealing temperature of 550 °C (curve d), in addition to the anatase features, a small peak emerged at $2\theta = 27.45°$, which can be assigned to the (110) diffraction plane of rutile TiO_2. At even higher annealing temperatures, this rutile peak became better defined (curve f). In fact, when the annealing temperature reached 600 °C, three additional peaks appeared at 36.09°, 44.05°, and 56.64°, which were consistent with the (101), (210), and (220) diffraction planes of rutile TiO_2, respectively. Concurrently, the anatase peaks became weakened, indicating that at these high annealing temperatures, an effective phase transformation occurred, resulting in the formation of a mixed crystal structure consisting of both anatase and rutile phases.[13]

Based on the Debye–Scherrer equation, the width of the anatase (101) diffraction peak was then used to estimate the average size of the anatase crystalline domains of the TiO_2 nanotubes, which was 25.6 nm at 400 °C, 28.6 nm at 450 °C, 34.2 nm at 500 °C, 32.6 nm at 550 °C, and 32.7 nm at 600 °C. The initial increase of the anatase domain size suggests enhanced crystallinity of the nanotubes with increasing temperature up to 450 °C, and at higher temperatures, the shrinking of the anatase domain size is due to the transformation of the anatase phase to the rutile counterpart, as it has been shown that at sufficiently high temperatures, large anatase grains of TiO_2 start to transform into rutile, whereas the small grains remain in the anatase form.[9]

FESEM measurements showed that the morphologies of the TiO_2 nanotube arrays remained practically unchanged with a deliberate control of the annealing
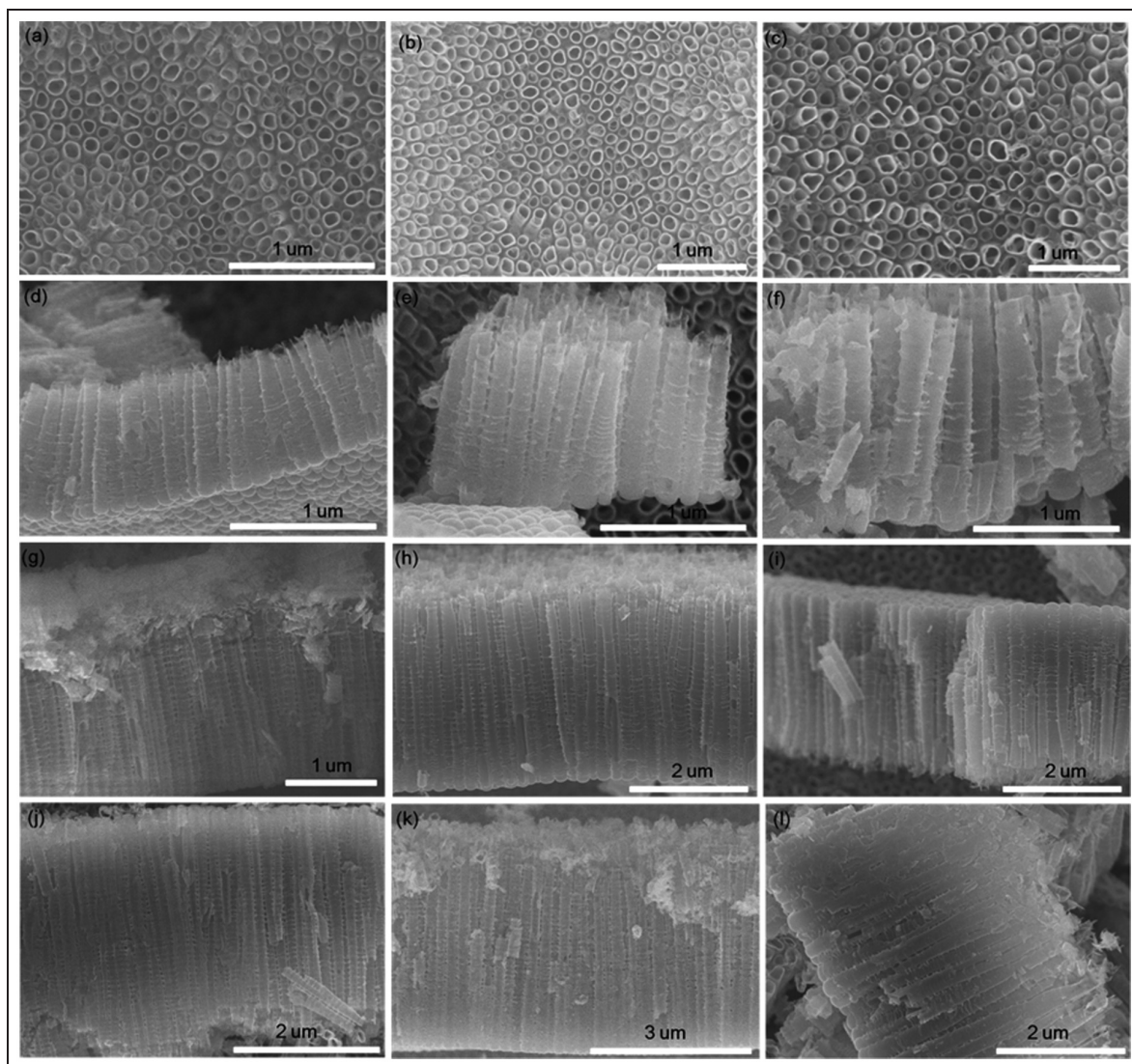
Figure 3. FESEM images of TiO$_2$ nanotubes arrays prepared at different applied voltages and anodization times. Images (a), (b), and (c) show the top views of TiO$_2$ nanotubes arrays prepared by anodization for 2 h at 25, 35, and 45 V, respectively. Images (d), (g), and (f) show the cross-sectional views of TiO$_2$ nanotubes arrays prepared at 25 V with the anodization time of 2, 10, and 12 h, respectively. Images (e), (h), and (k) show the cross-sectional views of TiO$_2$ nanotubes arrays prepared at 35 V with the anodization time of 2, 8, and 12 h, respectively. Images (f), (i), and (l) show the cross-sectional views of TiO$_2$ nanotubes arrays prepared at 45 V with the anodization time of 2, 6, and 12 h, respectively.

temperature. From Figure 5, one can see that in comparison to the as-prepared sample (panel a), after thermal annealing within the temperature range of 400 °C–550 °C (panels b to d), the samples maintained excellent thermal stability with a well-ordered tubular structure and only a smaller number of particulate fragments between the nanotubes.[15] At higher temperatures (600 °C, panel f), however, the nanotubes began to collapse and more recognizable particles and fragments appeared. Similar behaviors were observed for TiO$_2$ nanotubes prepared at other conditions (anodization voltage and reaction time).

The photocatalytic activity of the resulting TiO$_2$ nanotube arrays was then evaluated and compared by using the photodegradation of ARS as the illustrating example. Figure 6 shows the absorption spectra of an ARS solution under UV photoirradiation for varied periods of time in the (a) absence and (b) presence of TiO$_2$ photocatalysts prepared at 25 V for 10 h and then annealed at 450 °C for 3 h. The absorption peak at 260 nm can be assigned to the π–π* transition of the anthracene moiety, the peak at 335 nm to the n–π* transition of the carbonyl group, and the broad peak at 520 nm to the conjugation between O=C and the heterocyclic ring (Figure 1).[16] These features may be used for the quantitative assessment of the degradation of ARS catalyzed by the TiO$_2$ nanotubes. From panel (a) of Figure 6, it can be seen that in the absence of catalysts, the absorption profiles of ARS remained virtually unchanged under UV photoirradiation for up to 180 min. In sharp contrast, with the addition of TiO$_2$ nanotubes, the absorption features diminished drastically under UV illumination, indicating apparent
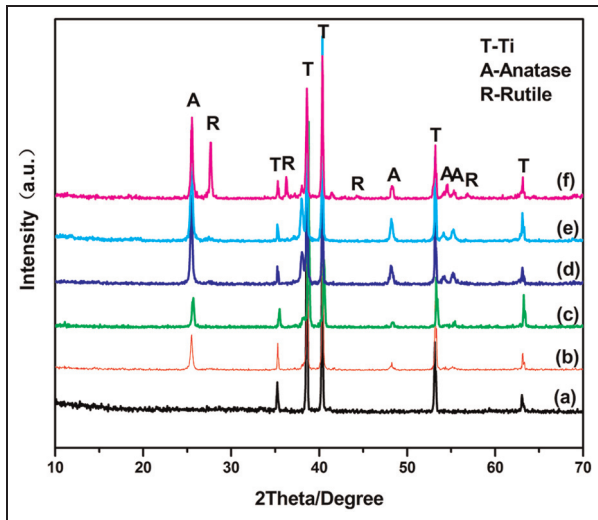
Figure 4. Representative XRD patterns of (a) TiO_2 nanotube arrays prepared at 25 V with the anodization time of 10 h and those thermally annealed at (b) 400 °C, (c) 450 °C, (d) 500 °C, (e) 550 °C, and (f) 600 °C.

photocatalytic activity of TiO_2 in the photodegradation of ARS.

The photocatalytic reactions catalyzed by TiO_2 nanotubes that were annealed at other temperatures were carried out in a similar fashion. The activity was quantified by monitoring the diminishment of the absorbance at 520 nm with photoirradiation time. The results are summarized in Figure 7. In panel (a), one can see that the fraction of ARS that remained in the solution (C_t/C_0) decreased exponentially with reaction time (t) for up to 180 min. From the linear profiles of $\ln(C_0/C_t)$ versus t, the first-order rate constants (κ) were then evaluated and listed in panel (b). It can be seen that for the TiO_2 nanotubes prepared by anodization at 25 V for 10 h, thermal annealing at 450 °C gave rise to the best photocatalytic activity with a rate constant of 2.70×10^{-3} min^{-1}. Similar behaviors can be observed with regard to the fraction of ARS that was photodegraded after 180 min of UV photoirradiation, which was 39.2%, the highest among the series. This coincides with the XRD measurements (Figure 4) where it was
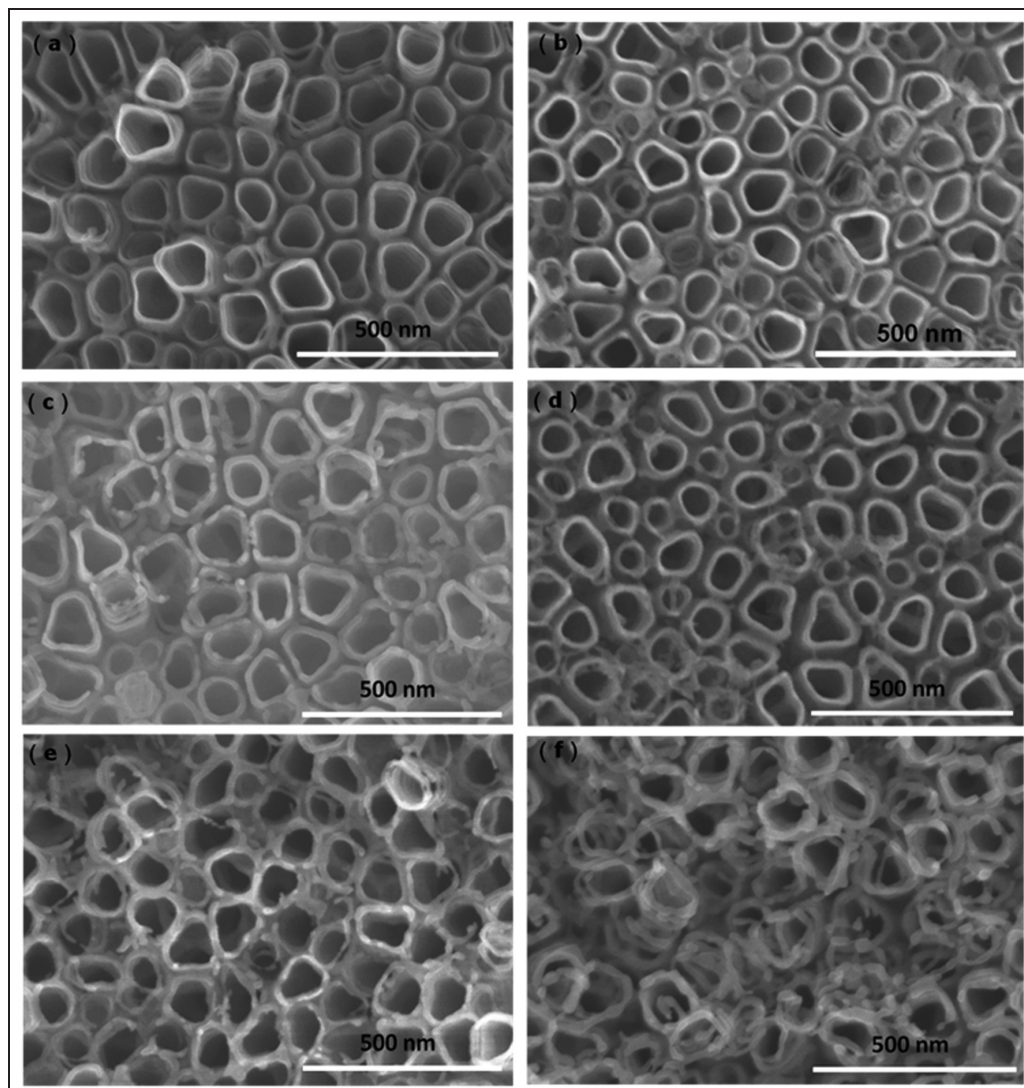

Figure 5. FESEM images of (a) TiO_2 nanotube arrays prepared at 25 V with the anodization time of 10 h and those thermally annealed at (b) 400 °C, (c) 450 °C, (d) 500 °C, (e) 550 °C, and (f) 600 °C. Scale bars all 500 nm.
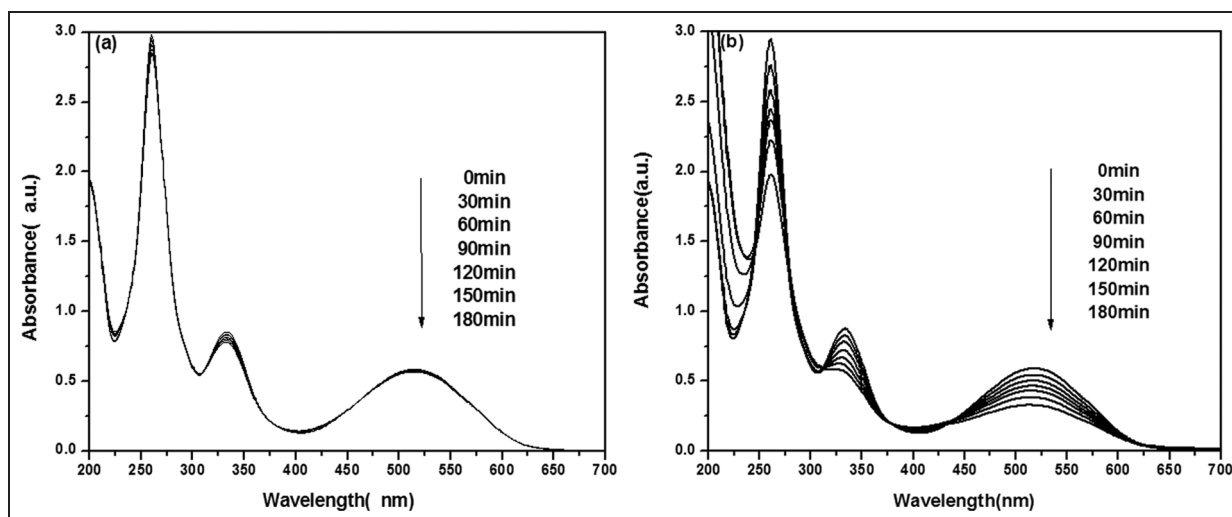
Figure 6. Representative UV-vis spectra of an ARS solution degraded (a) without and (b) with TiO$_2$ nanotube arrays (anodized at 25 V for 10 h and then annealed at 450 °C for 3 h) under UV light illumination.
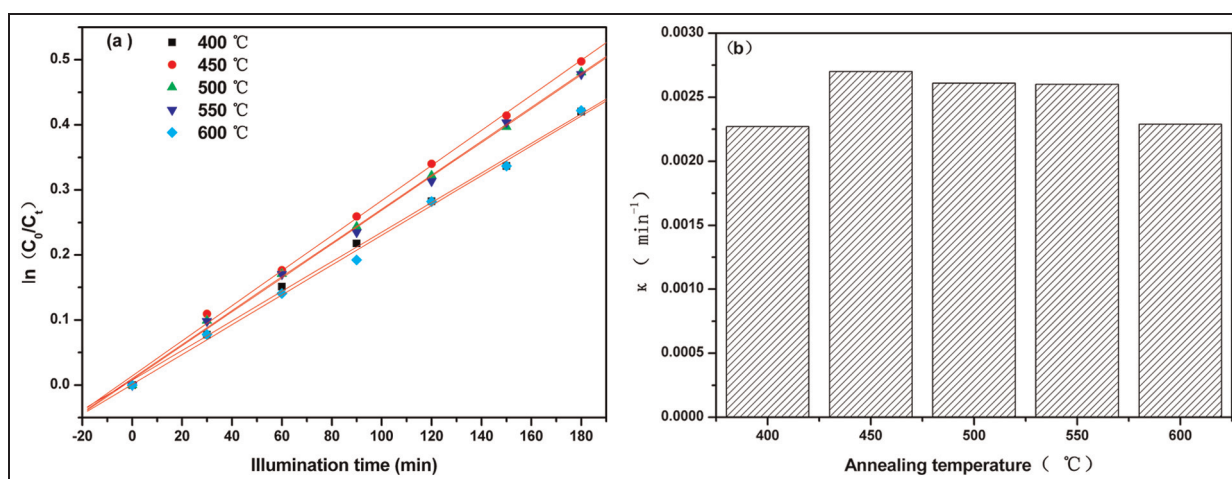

Figure 7. (a) Photocatalytic activity of TiO$_2$ nanotube arrays annealed at different temperatures (anodized at 25 V for 10 h and then annealed at various temperatures for 3 h), with the corresponding kinetic rate constants (κ) listed in panel (b).

shown that the anatase crystalline domain reached the maximum at this temperature, and anatase is known to be the optimal phase for photocatalysis.[17–19] The results highlight the significance of thermal annealing in manipulating the TiO$_2$ crystalline characteristics and hence the photocatalytic performance in the photodegradation of ARS.

A comparative study was carried out for other TiO$_2$ nanotubes that were also annealed at this temperature, and the results are summarized in Table 1. Interestingly, the photocatalytic activity might be further improved with a deliberate selection of preparative parameters. For instance, at the anodization voltage of 35 V, the best photocatalytic activity was observed with the samples prepared by anodization for 8 h, with a rate constant (κ) of 2.65×10^{-3} min^{-1} and 38.1% degraded after 180 min of UV illumination; whereas for the those prepared at 45 V, the optimal reaction time

was identified at 6 h, with a rate constant (κ) of 2.50×10^{-3} min^{-1} and 36.7% degraded after 180 min of UV illumination.

Taken together, these results suggest that within the present experimental context, the TiO$_2$ nanotube arrays prepared by anodization at 25 V for 10 h and then thermally annealed at 450 °C for 3 h exhibited the best photocatalytic activity in the degradation of ARS under UV photoirradiation. In addition to annealing temperatures that dictate the crystalline properties of the nanotubes, the dimensions and morphologies of the nanotubes appeared to play an important role as well with an optimal range of nanotube length, diameters, and surface density. As manifested in Figure 3, the nanotube pore size and length increased, whereas the number density on the Ti sheet decreased, with the increase of the anodization voltage and reaction time. Note that the specific surface area decreased with

Table 1. Summary of photocatalytic activity (first-order rate constant, κ, and fraction of ARS degraded after 180 min of UV photoirradiation, x) of TiO_2 nanotubes prepared at different anodization voltages for various periods of times.

	TiO_2	2 h	4 h	6 h	8 h	10 h	12 h
κ (10^{-3} min^{-1})	25 V	1.12	1.46	1.71	2.27	2.70	2.33
	35 V	1.29	2.05	2.11	2.65	2.34	2.11
	45 V	1.69	2.23	2.50	2.23	2.06	1.91
x (%)	25 V	18.7	23.6	26.8	34.1	39.2	35.2
	35 V	21.0	29.7	31.4	38.1	35.5	32.1
	45 V	26.7	33.9	36.7	33.6	30.7	29.6

Note that all samples were thermally annealed at 450 °C for 3 h.

increasing nanotube pore diameter; thus, a somewhat lower voltage is preferred for maximal surface accessibility.[20] Furthermore, it is interesting to note that of all the TiO_2 nanotubes under study, the optimal length is around 3 µm, as depicted in Figure S1 (Electronic Supplementary Information), where the decomposition rate constants (κ) exhibited a peak-shaped dependence on the nanotube length with the maximum at about 3 µm, regardless of the initial anodization voltage. This is likely a combined consequence of light penetration and hence absorption that drove the catalytic reactions, as well as mass transport of reactants and products within the nanotube arrays.[21]

Conclusion

Organized TiO_2 nanotube arrays were prepared by electrochemical anodization of titanium metal sheets. It was found that the nanotube pore diameter and length could be readily manipulated by the variation of the anodization voltage and reaction time, as manifested in SEM measurements. XRD studies showed that nanotube arrays thermally annealed at 450 °C exhibited the largest anatase crystal domains and hence best photocatalytic performance in the degradation of ARS under UV irradiation. Furthermore, the results indicated that the photocatalytic activity might be further improved by a deliberate variation of the nanotube dimensions which likely arose from the combined contributions of specific surface area and mass transport within the nanotube arrays.

Declaration of conflicting interests

The authors declared no potential conflicts of interest with respect to the research, authorship, and/or publication of this article.

Funding

References

1. Zhai T, Xie S, Zhao Y, et al. Controllable synthesis of hierarchical ZnO nanodisks for highly photocatalytic activity. *Cryst Eng Comm* 2012; 14(5): 1850–1855.
2. Zlamal M, Macak J, Schmuki P, et al. Electrochemically assisted photocatalysis on self-organized TiO_2 nanotubes. *Electrochem Commun* 2007; 9(12): 2822–2826.
3. Liu FZ, Shao X, Wang JQ, et al. Solvothermal synthesis of graphene-CdS nanocomposites for highly efficient visible-light photocatalyst. *J Alloys Compd* 2013; 551: 327–332.
4. Khalid NR, Hong ZL, Ahmed E, et al. Synergistic effects of Fe and graphene on photocatalytic activity enhancement of TiO_2 under visible light. *Appl Surf Sci* 2012; 258(15): 5827–5834.
5. Xiao N, Li Z, Liu J, et al. A facile template-free method for preparing bi-phase TiO_2 nanowire arrays with high photocatalytic activity. *Mater Lett* 2010; 64(16): 1776–1778.
6. Guo Y, Lee N-H, Oh H-J, et al. Preparation of titanate nanotube thin film using hydrothermal method. *Thin Solid Films* 2008; 516(23): 8363–8371.
7. Liu Y, Li J, Zhou B, et al. Comparison of photoelectrochemical properties of TiO_2-nanotube-array photoanode prepared by anodization in different electrolyte. *Environ Chem Lett* 2009; 7(4): 363–368.
8. Wu X, Jiang Q-Z, Ma Z-F, et al. Synthesis of titania nanotubes by microwave irradiation. *Solid State Commun* 2005; 136(9–10): 513–517.
9. Allam NK and El-Sayed MA. Photoelectrochemical water oxidation characteristics of anodically fabricated TiO_2 nanotube arrays: Structural and optical properties. *J Phys Chem C* 2010; 114(27): 12024–12029.
10. Toledo Antonio JA, Cortes-Jacome MA, Orozco-Cerros SL, et al. Assessing optimal photoactivity on titania nanotubes using different annealing temperatures. *Appl Catal B: Environ* 2010; 100(1–2): 47–54.
11. Kang XW and Chen S. Photocatalytic reduction of methylene blue by TiO_2 nanotube arrays: effects of TiO_2 crystalline phase. *J Mater Sci* 2010; 45(10): 2696–2702.
12. Yu J and Wang B. Effect of calcination temperature on morphology and photoelectrochemical properties of anodized titanium dioxide nanotube arrays. *Appl Catal B: Environ* 2010; 94(3–4): 295–302.

13. Lai Y, Zhuang H, Sun L, et al. Self-organized TiO_2 nanotubes in mixed organic–inorganic electrolytes and their photoelectrochemical performance. *Electrochim Acta* 2009; 54(26): 6536–6542.

14. Schulte KL, DeSario PA and Gray KA. Effect of crystal phase composition on the reductive and oxidative abilities of TiO_2 nanotubes under UV and visible light. *Appl Catal B: Environ* 2010; 97(3–4): 354–360.

15. Li G, Liu Z-Q, Lu J, et al. Effect of calcination temperature on the morphology and surface properties of TiO_2 nanotube arrays. *Appl Surf Sci* 2009; 255(16): 7323–7328.

16. Khosa MA, Shah SS and Nazar MF. UV-Visible spectrometric study and micellar enhanced ultrafiltration of Alizarin Red S dye. *J Dispersion Sci Technol* 2011; 32(11): 1634–1640.

17. Carp O, Huisman CL and Reller A. Photoinduced reactivity of titanium dioxide. *Prog Solid State Chem* 2004; 32(1–2): 33–177.

18. Demeestere K, Dewulf J and Van Langenhove H. Heterogeneous photocatalysis as an advanced oxidation process for the abatement of chlorinated, monocyclic aromatic and sulfurous volatile organic compounds in air: State of the art. *Crit Rev Env Sci Technol* 2007; 37(6): 489–538.

19. Chen Q and Peng LM. Structure and applications of titanate and related nanostructures. *Int J Nanotechnol* 2007; 4(1–2): 44–65.

20. Zhuang HF, Lin CJ, Lai YK, et al. Some critical structure factors of titanium oxide nanotube array in its photocatalytic activity. *Environ Sci Technol* 2007; 41(13): 4735–4740.

21. Liang H-C and Li X-Z. Effects of structure of anodic TiO_2 nanotube arrays on photocatalytic activity for the degradation of 2,3-dichlorophenol in aqueous solution. *J Hazard Mater* 2009; 162(2–3): 1415–1422.